Control of Giant Breathing Motion in C_{60} with Temporally Shaped Laser Pulses

T. Laarmann,[1,*] I. Shchatsinin,[1] A. Stalmashonak,[1] M. Boyle,[1,†] N. Zhavoronkov,[1] J. Handt,[2] R. Schmidt,[3] C. P. Schulz,[1] and I. V. Hertel[1,‡]

[1]*Max Born Institute, Max-Born-Strasse 2a, D-12489 Berlin, Germany*

[2]*Max Planck Institute for the Physics of Complex Systems, Nöthnitzer Strasse 38, D-01187 Dresden, Germany*

[3]*Institut für Theoretische Physik, Technische Universität Dresden, D-01062 Dresden, Germany*

(Received 13 October 2006; published 1 February 2007)

Femtosecond laser pulses tailored with closed-loop, optimal control feedback were used to excite oscillations in C_{60} with large amplitude by coherent heating of nuclear motion. A characteristic pulse sequence results in significant enhancement of C_2 evaporation, a typical energy loss channel of vibrationally hot C_{60}. The separation between subsequent pulses in combination with complementary two-color pump-probe data and time-dependent density functional theory calculations give direct information on the multielectron excitation via the t_{1g} resonance followed by efficient coupling to the radial symmetric $a_g(1)$ breathing mode.

DOI: 10.1103/PhysRevLett.98.058302 PACS numbers: 82.53.−k, 33.80.Wz, 61.48.+c

The control of photophysical processes with judiciously tailored femtosecond (fs) laser pulses is a cutting edge topic in modern laser science and might pave the way to optically controlled organic chemistry [1]. A great variety of pulse-shaping experiments has been performed since the concept of closed-loop, adaptive feedback control was proposed [2]. Efficient use of self-learning optimization algorithms allows one to control different photoinduced processes such as selective fragmentation [3], bond dissociation and rearrangement [4], laser-induced fluorescence [5], stimulated Raman emission [6], or high-harmonic generation [7]. The motivation behind this powerful method is mainly twofold: (i) to maximize a specific, selected reaction and (ii) to learn about the thus induced (optimized) process itself. The latter is usually very difficult to achieve for large finite systems with many electronic and nuclear degrees of freedom [8], in particular, if strong-field laser pulses are used which may be very efficient in reaching the former purpose [9].

In this Letter we report strong-field fs pulse-shaping experiments with C_{60} fullerenes which illustrate that both objectives may be approached in a complex manybody system. C_{60} may be regarded as a model system for studying the dynamics of energy deposition, redistribution, and coupling [10], and by controlling the molecular response with adaptive closed-loop feedback, fundamental questions can be addressed, such as to the role of intermediate electronic excited states in ionization and/or dissociation processes [11,12]. In particular, the interplay between single active electron (SAE) dynamics, which dominates the strong-field response of atoms, multi active electron (MAE) response expected in polyatomic molecules [13–16], and efficient coupling to nuclear degrees of freedom are of high current interest [17,18]. Here we focus on selective enhancement of C_2 evaporation, a typical energy loss channel of vibrationally excited fullerenes. The combination of optimal control with complementary 2-color pump-probe experiments and time-dependent density functional theory (TDDFT) allows us to pinpoint the "microscopic" process. We present evidence that due to a mechanism which may be called coherent heating of nuclear motion, the strong specifically shaped pulsed field induces multielectron excitation via the t_{1g} doorway state followed by efficient coupling to the $a_g(1)$ breathing mode of the nuclear backbone of C_{60}.

We use a 1 kHz Ti:sapphire laser system generating 800 nm pulses of 27 fs duration (FWHM) with a pulse energy of 800 μJ. The radiation passes a pulse former that consists of a liquid crystal modulator (Jenoptics SLM-S 640/12) placed in the Fourier plane of a zero dispersion compressor [19]. The computer controlled liquid crystal (LC) array of 640 pixels allows variation of the spectral phase function in the interval $(0–2\pi)$. Typically, the spectral phase was specified at 32 equidistant wavelengths and in between a spline interpolation was used to set the LC array. This turned out to be a good compromise for approximating the global maximum in solution space, while keeping the number of free parameters small and the convergence time short. The shaper setup has a total transmission of $\simeq 35\%$ and phase-only shaping implies constant pulse energy throughout the experiment. Its dispersion without applying a phase mask slightly broadens the pulse to 31 fs duration. The temporally shaped laser pulses were focused onto the molecular beam produced from C_{60} powder heated to 770 K. The waist of the focused beam was determined by the standard knife-edge method to be $w_0 = 58\ \mu$m (at $1/e$ of maximum intensity). Wave front measurements assure spatial uniformity of the light pulse during the optimization process. Ions generated at the intersection volume were extracted with a static electric field and recorded with a time-of-flight (TOF) mass spectrometer. Experimental details are reported elsewhere [20].

Finding the optimal pulse shape is done in analogy to similar optimization processes occurring in nature by a

feedback learning loop. From the different approaches possible [21] we used an evolutionary strategy by which we obtained robust optimal solutions with good convergence. We start with 20 randomly chosen phase masks (1st generation). The response of the molecular system is evaluated for each mask by recording a mass spectrum averaged over 1000 laser pulses. The two pulse shapes with the best fitness value, e.g., the C_{50}^+ ion counts, are carried over to the next generation without changes. The remaining 18 members of the new generation are created by *crossover* events, where the phase pattern from two randomly chosen masks are partially exchanged. In a second step the newly created members are modified in a *mutation* event, where with a 20% probability the pixels of the phase mask are replaced by a random value. Convergence is achieved after typically 30–40 generations. The resulting optimal pulse shape for a predefined target is characterized by cross-correlation frequency-resolved optical gating (SH-XFROG).

A typical learning curve for maximizing the C_{50}^+ fragment ion yield is plotted in Fig. 1(a), with the XFROG-trace of the corresponding optimal pulse shown in the inset. During the learning process the C_{50}^+ ion signal increased by a factor of $\simeq 2.4$ compared to the signal recorded with unshaped pulses (0th *generation*). The C_{50}^+ ion abundance was chosen as an optimization target because it is a measure for the temperature of the nuclear backbone. It is well known that cooling of highly vibrationally excited C_{60} occurs mainly through sequential evaporation of C_2 units in a statistical process [10]. Thus, a strong correlation of the optimization curve with those of the neighboring fragments C_{48}^+ and C_{52}^+ is observed (not shown here). It is important to note that our present control scheme does not optimize selective bond breaking. Rather, it maximizes the process of energy flow into vibrational modes of C_{60}. For comparison we have measured the C_{50}^+ with a stretched pulse of the same overall energy and duration [Fig. 1(c)] as our optimal pulse [Fig. 1(b)] and find the signal for the optimal pulse to be more than 2 times stronger. The ratios $R = C_{50}^+/C_{60}^+$ even increased by factors of 7 and 32 compared to those of the stretched and the unshaped pulse, respectively. These observations thus go far beyond the common wisdom according to which the response of fullerenes to intense laser fields is found to be determined by the pulse duration as recently reviewed [10]: the XFROG trace in Fig. 1(a) clearly shows that a sequence of pulses is best suited for most efficient energy coupling into nuclear motion. The wave packet generated by this pulse sequence prevails apparently for at least 6 cycles, surprisingly long considering the large number of electronic and nuclear degrees of freedom into which energy can finally flow.

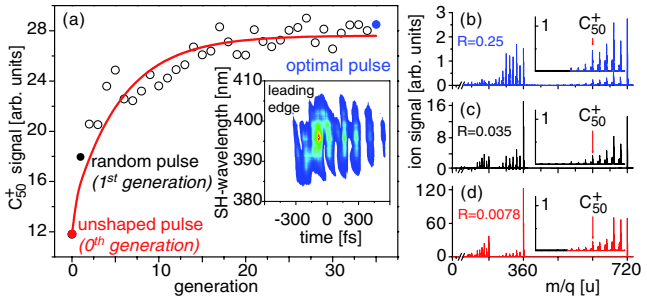

FIG. 1 (color online). (a) C_{50}^+ signal as a function of generation of the evolutionary algorithm. The inset shows the XFROG trace of the optimal solution. On the right, mass spectra recorded with optimal (b), stretched to 340 fs (c), and unshaped pulses of 31 fs FWHM are plotted. The ratios $R = C_{50}^+/C_{60}^+$ are given.

To corroborate these findings and to glean further insight into the underlying manybody dynamics we performed complementary 2-color pump-probe experiments with a relatively weak frequency-doubled 400 nm pump pulse, resonant with the dipole-allowed HOMO(h_u) $\rightarrow$ LUMO + 1(t_{1g}) transition, assumed to mimic essentially the excitation effect of the leading edge of the strong, shaped 800 nm pulse in the previous experiment. The dynamics of the energy redistribution is then probed by a time-delayed 800 nm probe pulse. Figure 2(a) shows the metastable C_{48}^{3+} ion signal as a function of the time-delay between 400 nm pump (1.7×10^{13} W/cm^2) and 800 nm probe pulse (7.3×10^{13} W/cm^2) with pulse durations of 25 and 27 fs, respectively. Triply charged, large fragments are most abundant using fs pulses as visible in Fig. 1(d) and metastable fragmentation (on a μs-ms time scale) is a particularly sensitive probe of the temperature of C_{60}^{q+} generated in the initial photoabsorption process [10]. At negative time delay, when the red pulse leads, almost no signal from C_{48}^{3+} is observed. Once pump and probe pulse overlap, the ion yield increases strongly and a maximum fragment signal is found at a delay of $\simeq$50 fs. It can be inferred from this observation that the resonant preexcitation of the LUMO + 1(t_{1g}) state by the blue laser pulse

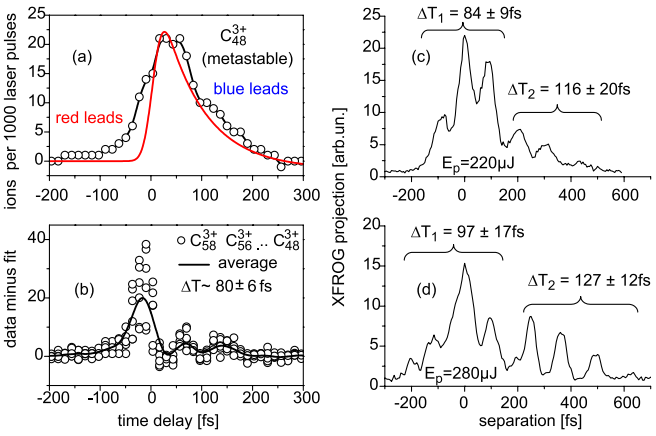

FIG. 2 (color online). (a) Metastable C_{48}^{3+} ion signal as a function of time delay between the blue pump and red probe pulse. An exponential decay is fitted to the data. (b) A modulation is found for all large fragments C_{60-2m}^{3+} by subtracting the fits from the measured transients. (c) Optimized temporal shape with 220 μJ laser pulses and (d) 280 μJ pulses.

significantly enhances multiple ionization and massive fragmentation both induced by the subsequent red pulse. The t_{1g} state has already been identified as the doorway state for the population of Rydberg states in C_{60} [22] and it seems to act generally as a bottleneck for photophysical energy deposition into C_{60}.

Closer inspection of the pump-probe transient reveals a weak modulation on top of the C_{48}^{3+} ion signal. By fitting the data to the laser cross-correlation function convoluted with a single exponential function decay and subtracting this from the measured signal, this modulation—albeit small—is found in all pump-probe data from multiply charged large fragments with a period of 80 ± 6 fs. This is shown in Fig. 2(b). Obviously, nuclear rearrangement upon electronic excitation via the t_{1g} state occurs. The oscillation is then probed by the 800 nm probe pulse, assuming (by virtue of Franck-Condon arguments) that the absorption cross section for further energy deposition depends on the C_{60} oscillation.

The comparison of the pump-probe modulation with results from pulse-shaping experiments [Fig. 1(a)] gives evidence that these different spectroscopic techniques probe very similar dynamics. Figures 2(c) and 2(d) show for comparison the optimal temporal shapes for excitation with 220 μJ and 280 μJ pulses, respectively, derived by projecting the XFROG-traces onto the time axis. The key findings reproduced in several optimization runs are as follows: (i) Each pulse shape consists of two distinct regimes with periodicity T_1 and T_2. (ii) The periodicity is smaller on the leading edge of the pulse than on the trailing edge ($T_1 < T_2$). (iii) It increases with increasing pulse energy. The observed values range from $T_1 = 84 \pm 9$ fs at 220 μJ up to $T_2 = 127 \pm 12$ fs at 280 μJ. All observed times including the pump-probe result are much larger than the well-known radially symmetric breathing mode $a_g(1)$ of neutral C_{60} molecules, which has an experimentally determined period of 67 fs [23]. On the other hand, the observed periods are in general shorter than the lowest prolate-oblate mode $h_g(1)$ (122 fs [23]) recently suggested as the dominantly excited mode of C_{60} due to the strong laser-induced dipole forces acting in intense 1500 nm pulses [24].

To glean information on the nuclear motion excited in strong 400 nm and 800 nm laser fields we used the so-called nonadiabatic quantum molecular dynamics (NA-QMD) [25], developed recently. In this approach, electronic and vibrational degrees of freedom are treated simultaneously and self-consistently by combining time-dependent density functional theory (TDDFT) in basis expansion with classical molecular dynamics. The NA-QMD theory has already been successfully applied to excitation and fragmentation mechanisms in ion-fullerene collisions [26] and laser-induced molecular dynamics [27–29]. In the present studies the adiabatic LDA functional is used. We note that the calculations are limited due to the computational effort by using the frozen core approximation and only a minimal basis set (i.e., $2s$, $2p_x$, $2p_y$, $2p_z$ orbitals) and, thus, describing the ionization mechanism not very realistically. However, in principle, it is possible to include realistically the ionization process in NA-QMD, demanding however many more basis functions and a reliable absorber potential [30].

In Fig. 3 we present the first results for excitating C_{60} by an intense laser field ($\lambda = 370$ nm, $\tau = 27$ fs) at different intensities. The wavelength of 370 nm is close to the experimentally used 400 nm pump pulse and matches the first optical resonance calculated with our method. The calculations shown in Fig. 3(a) predict an efficient excitation of many electrons by the laser field. At the highest laser intensity (5×10^{13} W/cm^2) nearly 31 valence electrons are strongly excited resulting in an impulsive force that expands the molecule dramatically up to 9.4 Å which is 130% of the C_{60} diameter, orders of magnitude larger than expected for any standard harmonic oscillation. At high laser intensities most of the kinetic energy of the nuclei is stored in the radially symmetric breathing mode $a_g(1)$ in contrast to the rather small contribution of the other vibrational modes as shown in Fig. 3(b) (calculated by analyzing the kinetic energy in normal modes) in agreement with other theoretical work [17]. The new equilibrium position as well as the oscillation period of the $a_g(1)$ depend on the excited electronic configuration, and, thus, on the absorbed energy. Figure 3(a) shows a strong increase of the oscillation period with increasing absorbed energy as observed experimentally. The calculated oscillation period of highly excited C_{60} is in good agreement with the results of the pump-probe experiment in Fig. 2(b) as well as with the first time regime of the optimally shaped laser pulse given in Figs. 2(c) and 2(d). The longer period seen experimentally in the second time regime are not reproduced by the theory, possibly due to the lack of absorbing boundary conditions

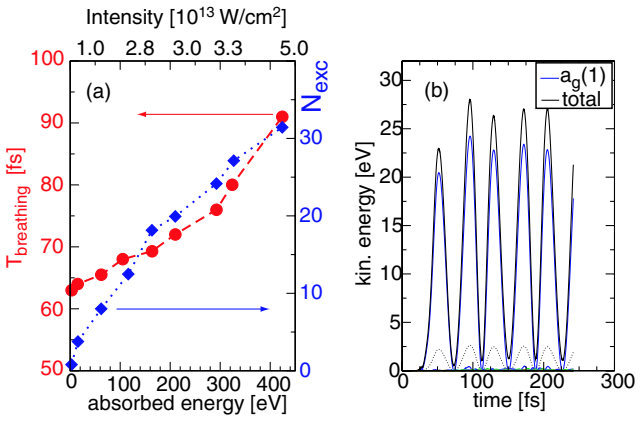

FIG. 3 (color online). (a) Period of the $a_g(1)$ breathing mode (circles) and number of excited electrons (diamonds) as a function of deposited energy derived from NA-QMD simulations (laser parameters: $\lambda = 370$ nm, $\tau = 27$ fs). (b) Vibrational energy of normal modes after laser excitation ($I = 3.3 \times 10^{13}$ W/cm^2). The kinetic energy is mainly stored in the $a_g(1)$ mode.

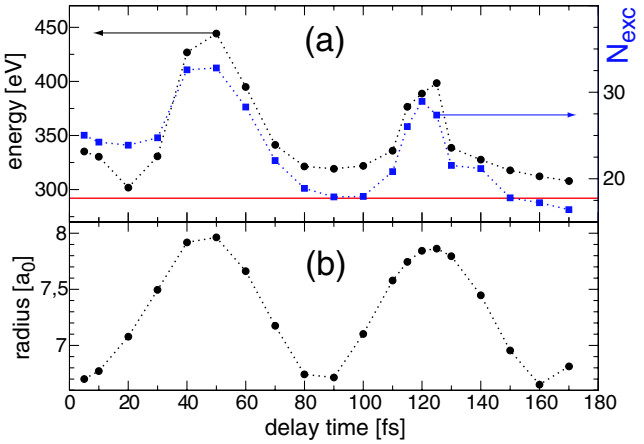

FIG. 4 (color online). (a) Absorbed energy (circles) and number of excited electrons (squares) of C_{60} after excitation with pump ($\lambda = 370$ nm, $I = 3.3 \times 10^{13}$ W/cm^2, $\tau = 27$ fs) and probe pulses ($\lambda = 800$ nm, $I = 7.3 \times 10^{13}$ W/cm^2, $\tau = 27$ fs) as a function of time delay. The horizontal line indicates the absorbed energy after the pump pulse alone (292 eV). (b) C_{60} radius at the maximum of the probe pulse as a function of delay time.

[30], since the breathing mode period of ionized C_{60} is increased in comparison with the neutral molecule. We also have simulated the pump-probe experiment by calculating the total absorbed energy as well as the radius as a function of the pump-probe delay time. Figure 4 shows a significant correlation between the actual radius, e.g., the $a_g(1)$ mode of the excited C_{60} with $T = 75$ fs, and the energy deposited after the probe pulse, which is the key for understanding the experimental observation.

To summarize, temporally shaped fs laser pulses with closed-loop, optimal control feedback were used to obtain detailed information on ultrafast electronic and nuclear dynamics in photoexcited C_{60} molecules. A characteristic pulse sequence was found to excite large-amplitude oscillations by coherent heating of nuclear motion. Complementary 2-color pump-probe studies allow us to identify the t_{1g} state to play the key role in the energy deposition process. With the help of TDDFT calculations we have been able to connect the experimentally observed periods and the calculated, laser-induced giant vibrational motion. A strong optical laser field excites many electrons in C_{60} fullerene via the t_{1g} doorway state. The almost homogenously distributed excited electron cloud couples to the radially symmetric $a_g(1)$ breathing mode. The observed period (80–127 fs) depends on the number of excited electrons (deposited energy) and the degree of ionization. Despite various electronic and nuclear degrees of freedom, this essentially one-dimensional motion prevails for up to 6 cycles with an oscillatory amplitude of up to 130% of the molecular diameter.

Financial support from the Deutsche Forschungsgemeinschaft through Sonderforschungsbereich 450 TP A2 is gratefully acknowledged.

*Corresponding author.
Electronic address: laarmann@mbi-berlin.de
†Present address: Laser Zentrum Hannover, Hollerithallee 8, D-30419 Hannover, Germany.
‡Also at: Department of Physics, Free University, Berlin, Germany.

[1] *Laser Control and Manipulation of Molecules*, edited by A. D. Bandrauk, Y. Fujimura, and R. J. Gordon, ACS Symposium Series Vol. 821 (Oxford University, Oxford, 2002).
[2] R. S. Judson and H. Rabitz, Phys. Rev. Lett. **68**, 1500 (1992).
[3] A. Assion *et al.*, Science **282**, 919 (1998).
[4] R. J. Levis, G. M. Menkir, and H. Rabitz, Science **292**, 709 (2001).
[5] C. J. Bardeen *et al.*, Chem. Phys. Lett. **280**, 151 (1997).
[6] T. C. Weinacht, J. L. White, and P. H. Bucksbaum, J. Phys. Chem. A **103**, 10 166 (1999).
[7] R. Bartels *et al.*, Nature (London) **406**, 164 (2000).
[8] J. Herek *et al.*, Nature (London) **417**, 533 (2002).
[9] R. J. Levis and H. A. Rabitz, J. Phys. Chem. A **106**, 6427 (2002).
[10] I. V. Hertel, T. Laarmann, and C. P. Schulz, Adv. At. Mol. Opt. Phys. **50**, 219 (2005).
[11] W. Fuss, W. E. Schmid, and S. A. Trushin, J. Chem. Phys. **112**, 8347 (2000).
[12] M. Murakami *et al.*, Chem. Phys. Lett. **403**, 238 (2005).
[13] B. Torralva *et al.*, Phys. Rev. B **64**, 153105 (2001).
[14] G. P. Zhang, X. Sun, and T. F. George, Phys. Rev. B **68**, 165410 (2003).
[15] M. Lezius *et al.*, Phys. Rev. Lett. **86**, 51 (2001).
[16] A. N. Markevitch *et al.*, Phys. Rev. A **69**, 013401 (2004).
[17] G. P. Zhang and T. F. George, Phys. Rev. Lett. **93**, 147401 (2004).
[18] J. Hauer, T. Buckup, and M. Motzkus, J. Chem. Phys. **125**, 061101 (2006).
[19] A. M. Weiner, Rev. Sci. Instrum. **71**, 1929 (2000).
[20] M. Boyle *et al.*, Eur. Phys. J. D **36**, 339 (2005).
[21] S. Schulze-Kremer, *Molecular Bioinformatics: Algorithms and Applications* (de Gruyter, Berlin, 1995).
[22] M. Boyle *et al.*, Phys. Rev. A **70**, 051201 (2004).
[23] Z. H. Dong *et al.*, Phys. Rev. B **48**, 2862 (1993).
[24] V. R. Bhardwaj, P. B. Corkum, and D. M. Rayner, Phys. Rev. Lett. **91**, 203004 (2003).
[25] T. Kunert and R. Schmidt, Eur. Phys. J. D **25**, 15 (2003).
[26] T. Kunert and R. Schmidt, Phys. Rev. Lett. **86**, 5258 (2001).
[27] T. Kunert, F. Grossmann, and R. Schmidt, Phys. Rev. A **72**, 023422 (2005).
[28] M. Uhlmann, T. Kunert, and R. Schmidt, Phys. Rev. A **72**, 045402 (2005).
[29] J. Handt, T. Kunert, and R. Schmidt, Chem. Phys. Lett. **428**, 220 (2006).
[30] M. Uhlmann, T. Kunert, and R. Schmidt, J. Phys. B **39**, 2989 (2006).